Nuclear Engineering and Design 435 (2025) 113960

Contents lists available at ScienceDirect

Nuclear Engineering and Design

journal homepage: www.elsevier.com/locate/nucengdes

PuMMA blind benchmark: Performance of high plutonium content MOX fuel under irradiation☆

D. Jaramillo-Sierra [a,b], M. Stefanowska-Skrodzka [c], J. Lavarenne [c], E. Deveaux [d], E. Brunetto [e], V. Matocha [f], A. Magni [a], K. Sturm [g], K. Mikityuk [h], Y. Wang [h], A. Jiménez-Carrascosa [h], J. Gado [i], B. Burger [i], V. Blanc [d], V. Dupont [d], L. Argeles [j], B. Perrin [k], G. Michel [k], A. Scolaro [e], C. Fiorina [e,o], J. Peltonen [l], A. Del Nevo [b,*], L. Luzzi [a], D. Pizzocri [a], S. Lemehov [m], S. Bebjak [n], T. Chrebet [n], C. Strmensky [n]

[a] Politecnico di Milano, Department of Energy, Nuclear Engineering Division, via La Masa 34, 20156 Milano, Italy
[b] ENEA, NUC-ING, Località Bacino del Brasimone 1, Camugnano 40032 Bologna, Italy
[c] Jacobs, Kings Point House, Queen Mother Square, Poundbury, Dorchester DT1 3BW, UK
[d] Commissariat à L'énergie Atomique et aux Énergies Alternatives – Cadarache, 13108 Saint-Paul-lez-Durance, France
[e] École Polytechnique Fédérale de Lausanne, Route Cantonale, 1015 Lausanne, Switzerland
[f] Ústav Jaderného Výzkumu Řež, Hlavní 130, 250 68 Husinec-Řež, Czech Republic
[g] Karlsruhe Institute of Technology, Hermann-von-Helmholtz-Platz 1, 76344 Eggenstein-Leopoldshafen, Germany
[h] Paul Scherrer Institute, Forschungsstrasse 111, 5232 Villigen, Switzerland
[i] EK-CER, 1-3 Konkoly-Thege Miklós út, 1121 Budapest, Hungary
[j] Électricité de France (EDF), 22-30 Avenue de Wagram, 75008 Paris, France
[k] FRAMATOME, Tour AREVA, 1 Place Jean Millier, 92400 Courbevoie, France
[l] VTT Technical Research Centre of Finland, Kivimiehentie 3, FI-02044 Espoo, Finland
[m] Belgian Nuclear Research Centre SCK·CEN, Boeretang 200, 2400 Mol, Belgium
[n] VUJE, Okružná 5, 918 64 Trnava, Slovakia
[o] Department of Nuclear Engineering, Texas A&M University, 423 Spence St, College Station, TX 77843, USA

ARTICLE INFO

Keywords:
Fuel performance
Code benchmark
High plutonium mixed-oxide fuel
Irradiation
CAPRIX
TRABANT-1/1
TRABANT-2/2

ABSTRACT

This paper presents the results of the first phase of the benchmark exercise in the PuMMA project, aimed at extending the reliability of fuel performance codes for Mixed Oxide (MOX) fuels with high plutonium content. The exercise involved the simulation of three irradiation experiments: (1) CAPRIX (45 % of Pu) carried out in the PHENIX reactor in France, (2) TRABANT1 (45 % of Pu) and (3) TRABANT2 (40 % of Pu) irradiated in the HFR reactor in The Netherlands. Thirteen organizations from nine countries participated, using eight different fuel performance codes. In this phase, besides the fuel specifications, boundary conditions such as linear heat rate, irradiation history, and cladding external temperature were provided. In a "blind" exercise, all codes were free to choose suitable models and correlations for the simulation without access to the experimental results. The main results of the "blind" phase are performed along with a sensitivity analysis to investigate the impact of various uncertainties on measurements, irradiation and input parameters. Significant discrepancies were observed among the different codes, attributed to the use of heterogeneous reference correlations and the absence of suitable models for some MOX-specific phenomena. Finally, insights are offered for the second phase of the benchmark, where the fuel performance codes' capabilities will be assessed against experimental results from Post-Irradiation Examinations of all three pins.

1. Introduction

The development of Generation-IV nuclear reactors utilizing Mixed

☆ This article is part of a special issue entitled: 'alternative fuels' published in Nuclear Engineering and Design.

* Corresponding author.
E-mail address: alessandro.delnevo@enea.it (A. Del Nevo).

https://doi.org/10.1016/j.nucengdes.2025.113960
Received 7 October 2024; Received in revised form 13 February 2025; Accepted 25 February 2025
Available online 5 March 2025
0029-5493/© 2025 The Authors. Published by Elsevier B.V. This is an open access article under the CC BY license (http://creativecommons.org/licenses/by/4.0/).

Nomenclature

FGR	Fission Gas Release
FPC	Fuel Performance Code
FR	Fast Reactor
HFR	High Flux Reactor
JOG	Joint Oxyde-Gaine
LFR	Lead Fast Reactor
LHR	Linear Heat Rate
LWR	Light Water Reactor
MOX	Mix Oxide
MTR	Material Test Reactor
PIE	Post Irradiation Examination
PuMMA	Plutonium Management for More Agility
WWER	Water-Water Energetic Reactor

Oxide (MOX) fuels with high plutonium (Pu) content offers significant potential for safer, more efficient and sustainable nuclear energy production. However, this advancement also presents unique challenges that must be addressed. Understanding the complexities associated with high Pu content MOX fuels in fast reactors (FRs) is essential for enhancing the readiness level of this technology as well as ensuring optimal safety and performance.

A primary challenge lies in extending the validity range of current fuel performance codes (FPCs) to accurately model the behavior of these advanced fuels. Existing FPCs are predominantly developed and validated for UO2 and – marginally – with lower Pu content fuels, these codes require research efforts to capture the fuel behavior for higher Pu contents, especially at high burnups. Addressing this need is essential for reliable prediction of fuel performance under diverse operating conditions in next-generation reactors.

The current absence of operating FRs in Europe, coupled with limited availability of Material Test Reactors (MTRs) capable of reproducing fast irradiation conditions, poses additional challenges. These constraints require reliance on past irradiation experiments. In this context, the PuMMA project aims to uncover past European irradiation experiments that explored high Pu content in MOX fuel under fast irradiation conditions (PUMMA).

1.1. PuMMA project overview

The PuMMA (Plutonium Management for More Agility) Project is an EU-funded initiative designed to redefine how plutonium is managed in Generation IV nuclear reactors. It aims to benchmark and enhance FPCs for high Pu content MOX fuels by systematically comparing them with experimental data. Unlike previous studies focusing on MOX fuels with 15–30 % of plutonium, this project investigates fuels with plutonium content reaching 40–45 %, which presents unique challenges and opportunities for reactor safety and performance (PUMMA).

1.2. Blind benchmark objectives and methodology

Within the PuMMA project the aim of Working Package 2 is to study the behavior of fuel in FRs under high plutonium content conditions. The project focuses on three experimental uranium–plutonium MOX fuel pins: CAPRIX (45 % of Pu), TRABANT1 (45 % of Pu) and TRABANT2 (40 % of Pu).

This benchmark study involves the use of various FPCs to extend their validity domain by simulating the three previously mentioned fuel pins. It is divided into two phases:

1. **Code-to-Code Comparison**: This initial phase involves comparing the outputs of different FPCs without prior knowledge of experimental results.
2. **Experimental Data Comparison**: The second phase validates the FPCs against experimental data obtained from post-irradiation examinations (PIEs) of the fuel pins.

The first phase, presented in this work, is a “blind” code-to-code comparison involving thirteen organizations from nine countries who participated, using eight different FPCs. Each participant received only the input data without any experimental results, allowing them to choose the models and correlations most suitable for FR MOX simulations. This phase is key for identifying the main variations between the different codes without bias from prior experimental knowledge. To further investigate the sources of these discrepancies, a complementary sensitivity analysis (detailed in Section 5) is conducted, assessing the impact of different modeling choices on the benchmark results (presented in Section 4). This analysis highlights which models and correlations contribute most to the observed variations, guiding improvements for the second phase.

All participants received a complete set of specifications, including details about the fuel and cladding geometries and properties. The boundary conditions provided were:

- Linear Heat Rate (LHR)
- Neutronic flux
- Cladding external temperature

These boundary conditions were supplied for each fuel pin at every timestep and axial position. The expected outcomes focused on comparing the performance of various codes under uniform input conditions. The blind nature of this phase allowed for the identification of discrepancies and areas needing improvement. These findings are insightful for the second phase of the benchmark, which will validate the models against experimental results and address issues identified in the first phase.

2. Irradiation experiments

The following section provides a detailed description of the irradiation experiments considered in this benchmark, outlining their specifications and relevance to the extension of the validation of FPCs. Table 1 summarizes the key specifications of the irradiation experiments considered in this study. These experiments were selected based on their high Pu content, relevant irradiation conditions, and availability of high-quality PIE data, which is essential for model and integral code validation. A particularly significant feature of this dataset is the inclusion of two fuel pins irradiated in a MTR, in addition to the one irradiated in a FR. During the second phase of the benchmark, this will enable a comparative analysis of fuel behavior under distinct irradiation environments, facilitating an in-depth examination of the differences in performance between similar fuels subjected to MTR and FR conditions.

2.1. CAPRIX

The CAPRIX capsule was irradiated in the PHENIX reactor from the 49th to 53rd cycle for approximately 360 equivalent full power days (EFPD) from January 1995 to January 2006. It was then unloaded from the reactor in March 2006. Throughout the irradiation, the CAPRIX capsule was placed next to a control subassembly (Venard and Deveaux, 2021; Venard, 2021). The irradiation history and external cladding temperature are plotted in Fig. 1.

2.2. TRABANT-1/1 and TRABANT-2/2

The TRABANT (Transmutation and Burning of Actinides in TRIOX)

Table 1
Irradiation experiments specifications.

Pin specifications	CAPRIX	TRABANT-1/1	TRABANT-2/2
Reactor	PHENIX (FR)	HFR (MTR)	HFR (MTR)
Equivalent irradiation time (days)	620.4	296.5	74.1
Max. LHR (W/cm)	354.2	631.3	465.9
Max. Cladding temperature (K)	750	875.9	839.3
Max. Burnup (% FIMA)	12.8	12.6	2.1
Fuel type	MOX	MOX	MOX
Manufacturer	JRC	CEA	CEA
Active length (mm)	850	340	340
Fuel center hole diameter (mm)	2.0	2.5	2.39
Fuel pellet diameter (mm)	5.42	5.42	5.426
Initial gap width (mm)	0.115	0.115	0.112
Total porosity (%)	5.47	4.5	6.5
Oxygen to metal ratio	2.00	1.98	1.995
Heavy metal composition	U: 55 % Pu: 45 %	U: 55 % Pu: 45 %	U: 60 % Pu: 40 %
Cladding material	AIM1	15–15 Ti	15–15 Ti
Cladding outer diameter (mm)	6.55	6.55	6.55
Cladding inner diameter (mm)	5.65	5.65	5.65
Filler gas pressure (Bar)	1	1	1
Filler gas composition	He: 95 %, N2: 5 %	He: 95 %, Ar: 5 %	He: 100 %

series hosted the TRABANT-1/1 and −2/2 experiments. Both the irradiation tests were conducted in the High Flux Reactor in Petten. The fuel was contained inside a sodium capsule shielded from thermal neutron to demonstrate the concept of burning plutonium and transmuting minor actinides in fast breeder reactors. The TRABANT-1/1 irradiation was active from May 1995 until May 1996 for a total of 12 HRF irradiation cycles, stopped due to pin failure (Nindiyasari et al., 2022). The TRABANT-2/2 irradiation began in November 2001 and continued for two cycles: 01–11 and 01–12. Subsequently, the experiment was suspended and resumed only in 2005 for one more cycle, 05–06. Following this cycle, control neutron-radiography was performed, revealing extensive fuel displacement. The irradiation was therefore discontinued (Til et al., 2022). Both the TRABANT irradiation histories and external cladding temperatures are plotted in Fig. 2, while the experimental set-up and irradiation capsule are described schematically in Fig. 3.

3. Fuel performance codes description and assumptions Check participants

The benchmark exercise involved the work of 14 European organizations, including 8 FPCs.

- FEMAXI (**KIT**)
- FRED (**PSI**).
- FUROM (**EK-CER**).
- GERMINAL (**CEA**, **EDF** and **FRAMATOME**).
- MACROS (**SCK CEN**).
- OFFBEAT (**EPFL**).
- TRAFIC (**VTT**).
- TRANSURANUS (**ENEA**, **POLIMI**, **UJV** and **VUJE**).

The **FEMAXI** code is a 1.5-dimensional fuel performance tool designed for simulating thermal and mechanical behavior of fuel rods under normal and transient conditions (Okawa et al., 2015). It supports light water reactors (LWRs), sodium-cooled reactors, and it can simulate behavior in other reactor types like LFRs by adjusting temperature boundary conditions on the clad. FEMAXI models temperature distributions, fission gas release (FGR), stress evolution and material deformation processes, but it does not model Joint Oxyde-Gaine (JOG) formation.

The **FRED** code is being developed by PSI to simulate both fast and LWR fuel behavior under base and accident conditions (Mikityuk and Shestopalov, 2011; Tverberg, 2007). FRED models fuel temperature distribution, FGR, inner pressure and material deformations

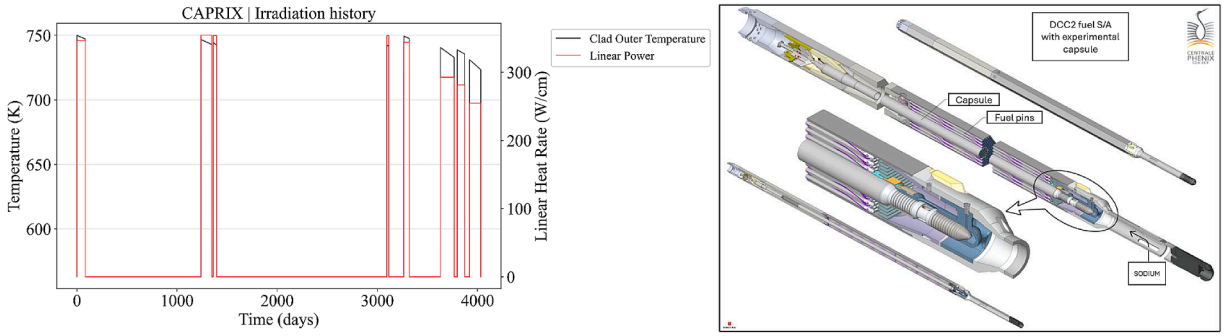

Fig. 1. CAPRIX Cladding nominal temperature and LHR at the peak power position (left) and schematic experimental set-up (right).

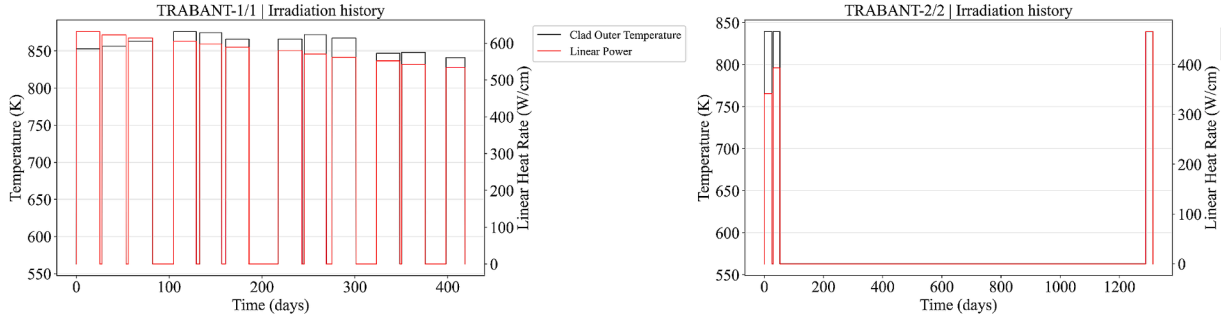

Fig. 2. TRABANT-1/1 (left) and −2/2 (right) Cladding nominal temperature and LHR at the peak power position.

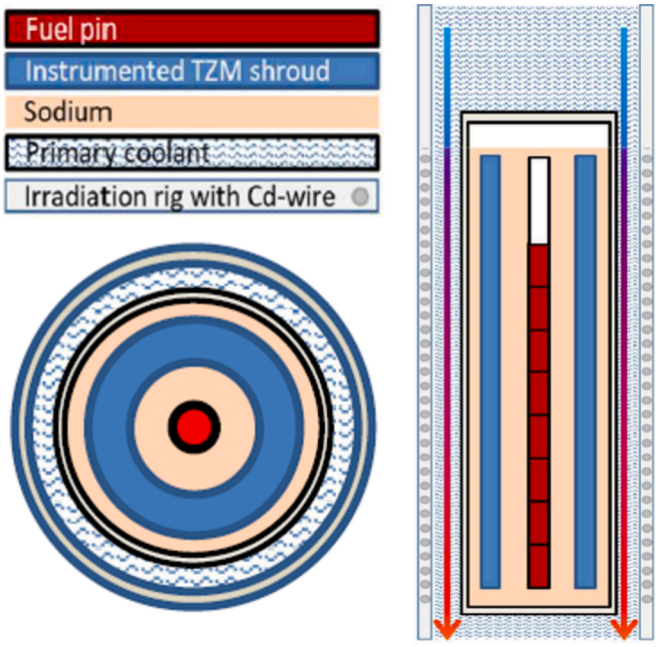

Fig. 3. TRABANT-1/1 and −2/2 Schematic experimental set-up and axial section of the sodium irradiation capsule.

(Philipponneau, 1992; Waltar and Reynolds, 1981; Hsieh et al., 1982; SCDAP/RELAP5-3D© Code Manual, 2003). The code lacks JOG modelling.

FUROM-FBR, developed by EK-CER, is used to simulate fuel behavior in FRs. Adapted from a code initially developed for WWER reactors, FUROM-FBR includes mechanistic models for material migration and FGR but lacks extensive FR validation due to the scarcity of experimental data.

The **GERMINAL** code, part of the PLEIADES platform (Lainet et al., 2019), simulates in-pile behavior of mixed oxide fuel in sodium-cooled FRs (Lainet et al., 2019). Developed by CEA, it integrates mechanistic models for neutron reactions, FGR and fuel restructuring. GERMINAL benefits from a large validation database, making it highly robust for fuel behavior predictions (Sundman et al., 2016; http://www-cast3m.cea.fr/).

MACROS, developed for the modelling of non-standard mixed oxide fuels, includes modules for fuel depletion, material property simulation and in-pile behavior. It simulates a wide range of fuel behaviors, including FGR, corrosion and cracking. MACROS is particularly useful for analyzing fuels with high concentrations of minor actinides and other non-standard compositions.

OFFBEAT, developed by EPFL and PSI, is a multi-dimensional code based on OpenFOAM®. It simulates complex phenomena in fuel performance, including 2D/3D behavior and axisymmetric conditions. The code is parallelized for efficient computation and includes modules for thermal analysis, fuel and cladding behavior, and FGR (Scolaro et al., 2020).

TRAFIC, developed within Jacobs, is a mechanistic code that divides the fuel pin into axial slices and uses finite element analysis to model temperature, stress and strain distribution. TRAFIC is validated using experimental data from transient tests but lacks JOG formation modelling, focusing instead on plutonium behavior and porosity evolution (Lavarenne et al., 2019).

TRANSURANUS, developed by the JRC of the European Commission, is a widely used FPC for simulating both fast and LWR fuels. It features extensive models for thermal and mechanical behavior, covering phenomena such as fuel restructuring, fission gas behavior and high burn-up structure formation. It is notable for its flexible, modular framework and ability to simulate various fuel types (Lassmann, 1992; Magni et al., 2021; European Commission, 2021; OECD/NEA, 2020; Di Marcello et al., 2012; Di Marcello et al., 2014; Magni et al., 2020; Magni et al., 2021; Lemehov, 2020; Van Uffelen et al., 2020).

3.1. FPCs main differences

The FPC involved in this benchmark exercise differ in their specific capabilities, modelling scopes, and computational approaches. Most of the codes represent a 1.5D axisymmetric domain, while some have the capability to extend to 2D and 3D simulations. A key difference among the codes lies in their modelling of fuel behavior, particularly FGR. While some codes rely on empirical correlations derived from specific experimental databases, others implement mechanistic models, which provide a physics-based approach to gas behavior.

Another significant variation concerns the modelling of JOG formation, a phenomenon absent from some codes entirely. Furthermore, differences in the representation of material properties, such as thermal conductivity and melting points highlight the distinct methodologies adopted across codes. A detailed comparison of these material properties, including their sources and associated correlations, is provided in Appendix A.

Among these differences, a fundamental distinction arises from the validation and benchmarking of the codes. The availability and scope of experimental databases significantly influence the reliability and applicability of specific models. For instance, some codes have undergone extensive validation for LWR applications but have limited benchmarking for FRs. On the contrary, some codes on proprietary databases tailored exclusively for FR validation, which can restrict cross-comparability with other FPCs.

These variations underscore the diverse design philosophies guiding the development of each code. While some prioritize high-fidelity mechanistic modelling, others emphasize modularity and adaptability. Additionally, certain codes are optimized for specific reactor types and operational scenarios, further shaping their applicability and predictive capabilities.

4. Benchmark results

This section presents the simulation results for the benchmark analysis. To ensure clarity, certain post-processing choices were made. Specifically, irradiation times were standardized by only considering the active irradiation periods, excluding inter-cycle intervals. This approach ensures a more consistent comparison among the codes. Each code's reference simulations are first established as a baseline, which will later be compared against sensitivity analyses. Consequently, the plots presented in this section display vertical lines corresponding to the reactor's operational cycles, reflecting the transitions between irradiation and non-irradiation phases. This visualization provides a clear representation of the reactor's periodic operation and facilitates the interpretation of the results.

4.1. CAPRIX results

The temperature results (see Fig. 4) show significant variation across the different simulations, with a particularly widespread in values. FEMAXI produced the highest fuel temperatures, reaching 2500 K at the pellet center and 1790 K at the outer surface, while other codes reported temperatures up to 500 K lower. This substantial difference highlights the key variations in how each code models thermal behavior under comparable conditions. Specifically, FEMAXI predicts the highest fuel temperatures due to its lower gap conductivity, whereas GERMINAL exhibits lower temperatures due to a peak in gap conductivity. These temperature trends align with the fuel-cladding gap conductivity reported in Fig. 6, illustrating the important role of gap conductance in heat transfer. Additionally, differences in fuel thermal conductivity models further influence the temperature distribution, as lower thermal

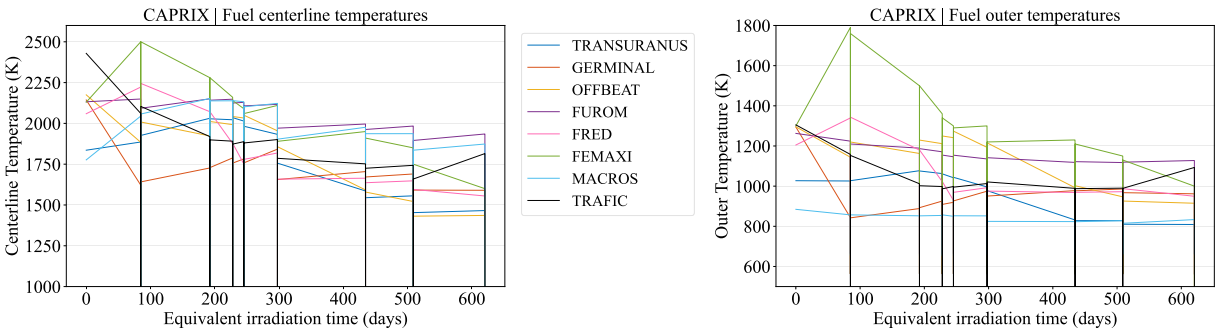

Fig. 4. CAPRIX Fuel centerline (left) and outer (right) temperatures at the peak power position.

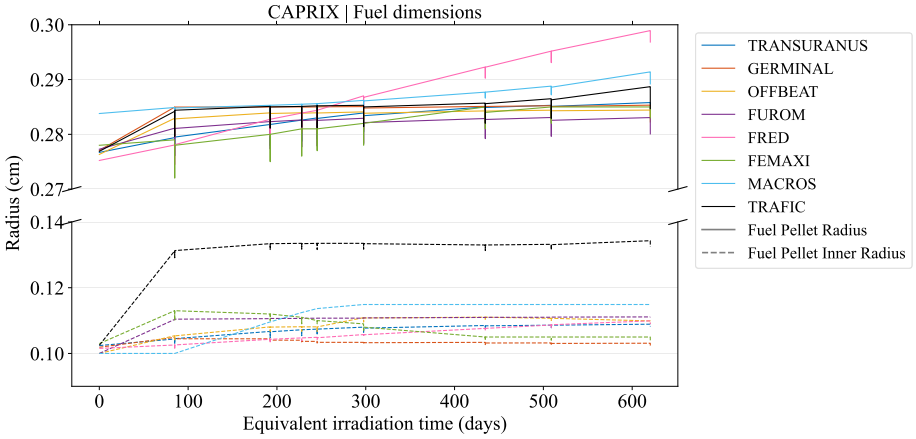

Fig. 5. CAPRIX Fuel outer and inner radius at the peak power position.

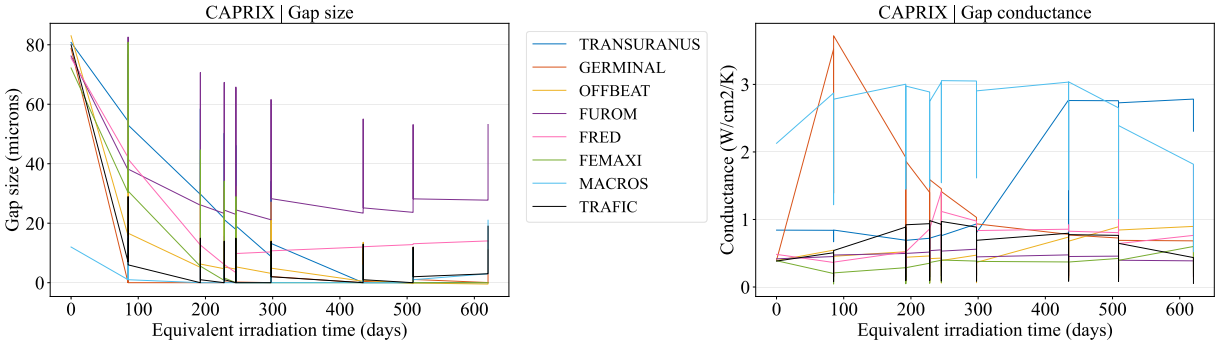

Fig. 6. CAPRIX Fuel-Cladding gap size (left) and gap conductance (right) at the peak power position.

conductivity may amplify the impact of the gap conductance by modeling lower heat dissipation within the pellet.

The increase in the fuel pellet outer radiuses is less spread, showing FRED as the only outlier that reaches a radius of 2.989 mm. The codes prediction of fuel inner radius evolution is linked with the temperature and even if is not the absolute highest values, TRAFIC code predicted the highest initial fuel temperature, therefore producing the highest restructuring values of 1.15 mm. Fig. 5 presents the CAPRIX fuel outer and inner radii at the peak power position, providing a detailed comparison of their evolution.

Fuel temperature is influenced by several parameters, including gap size and gap conductance. As expected, there is a significant spread between the gap conductance models (see Fig. 6). Looking at the fuel-cladding gap size, GERMINAL predicts an early gap closure compared to other codes, while FUROM predicts no gap closure at all. This behavior is reflected in the gap conductance, where some codes clearly model an increase in conductivity once contact between the fuel and cladding occurs. The observed discrepancies in gap closure can largely be attributed to differences in the fuel relocation models. The fuel relocation model of GERMINAL appears to drive its early gap closure prediction, potentially influencing its overall thermal response.

Despite the wide temperature variation across the codes, the FGR showed only two outliers: FRED predicted the highest release at 0.00036 m^3, suggesting that the FGR model implemented in FRED code should be reevaluated, while TRAFIC showed the lowest values. Contact pressure was negligible in most codes; however, FRED predicted extremely high values, likely due to the increase in the outer pellet radius. Codes such as FEMAXI and TRANSURANUS predicted more moderate contact pressures. These trends are further detailed in Fig. 7, which compares FGR predictions and contact pressure among the different codes.

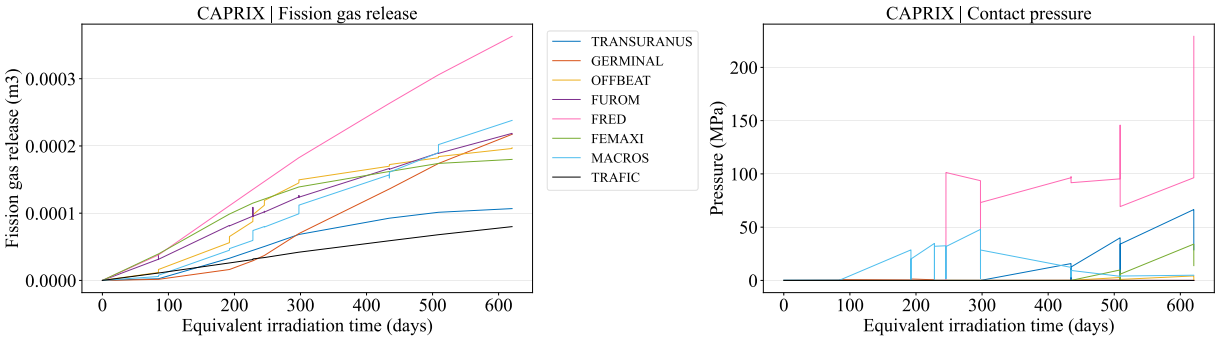

Fig. 7. CAPRIX FGR (left) and Fuel-Cladding contact pressure (right) at the peak power position.

4.2. TRABANT-1/1 results

Among the three fuel irradiations in this study, TRABANT-1/1 exhibits the highest values of LHR and cladding temperature. As anticipated, the centerline fuel temperature predicted by all codes also shows comparatively high values. The FRED code produced the highest centerline temperature, reaching 2881 K at the start of irradiation, approximately 300 K higher than the MACROS code, which yielded the lowest initial temperature. The outer pellet temperatures exhibit two distinct trends: during the first two cycles, most codes produced similar results, except for MACROS and TRANSURANUS. However, as irradiation progressed, the temperatures converged into two groups, primarily influenced by gap conductivity. This divergence is largely driven by variations in gap size and the fission gasses depredating the gap conductivity. Fig. 8 presents these trends, illustrating the TRABANT-1/1 fuel centerline and outer temperatures at the peak power position, highlighting the differences in predictions over the irradiation period.

The restructuring effects due to high temperatures and elevated LHR are evident in Fig. 9. The enlargement of the central hole is significant across all codes, especially for TRAFIC, which predicts an inner radius of 1.598 mm at the end of irradiation. The outer geometry of the fuel remains consistent among the codes, except for FRED, which shows a radial dimension of 2.99 mm, significantly higher than the other codes involved.

During the first cycle, all codes, except MACROS and FRED, exhibited similar trends in the reduction of gap size. Most codes predicted a gradual closure of the gap, except TRAFIC, which shows greater radial expansion of the cladding relative to the increase in pellet dimensions, therefore enlarging the gap size continuously. A strong fuel-cladding contact is predicted by three codes, with FRED estimating the maximum value. This can be seen in the gap conductivity trends (see Fig. 10).

Among the results analyzed, the FGR shows the greatest variability across the codes, with differences reaching an order of magnitude (see Fig. 11). These major discrepancies are attributable to modeling choices also influenced by the inherent complexity of FGR and how it is implemented in each code. Many of the correlations and models are based on LWR conditions and are highly sensitive to experimental coefficients, for which data is scarce, especially for MOX fuels at FR conditions.

4.3. TRABANT-2/2 results

The TRABANT-2/2 experiment has a shorter duration, so burn-up degradation phenomena appear less prominently across the different codes. All codes recorded the highest fuel temperatures during the third cycle, which is the overpower cycle. The absolute peak temperature was predicted by FRED, reaching 2821 K, while FEMAXI recorded the highest outer pellet temperature at 2000 K. Consistently, GERMINAL and MACROS predicted the lowest temperatures, as shown in Fig. 12, which can be attributed to early fuel-cladding gap closure in both codes.

The evolution of pellet geometry shows less variation compared to temperatures, with all codes following an aligned behavior, as shown in Fig. 13. The only outlier in this result is TRAFIC that predicted the largest inner radius, reaching 1.52 mm by the end of the third cycle and more than 0.2 mm higher than FEMAXI.

The increase in the outer pellet radius reduced the fuel-cladding gap, but only GERMINAL predicted full closure (see Fig. 14). This is also reflected in the conductance values, which rise significantly due to contact. None of the other codes predicted gap closure during the full irradiation of TRABANT-2/2.

The release of fission gases from the fuel matrix varied significantly among the codes according to results shown in Fig. 15. FEMAXI predicted the highest release, reaching 2.07e-05 m^3, while FRED showed the lowest. Consistent with the gap size, GERMINAL was the only code that predicted contact pressure, reaching 1.04 MPa.

5. Sensitivity analysis

In this section, the complementary sensitivity analysis is presented to further investigate the discrepancies observed in the benchmark results (Section 4). This analysis assesses the impact of different input

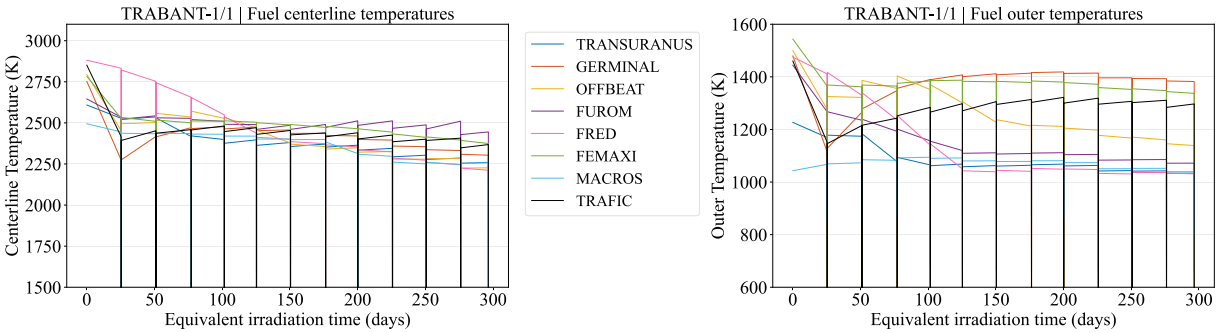

Fig. 8. TRABANT-1/1 Fuel centerline (left) and outer (right) temperatures at the peak power position.

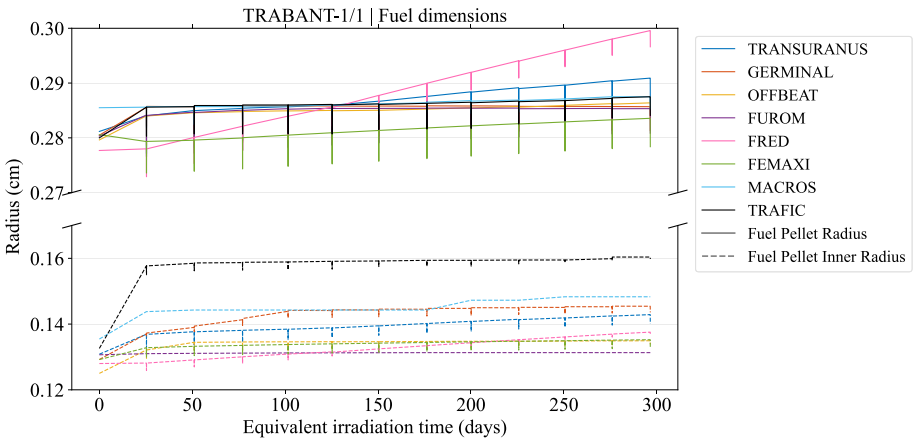

Fig. 9. TRABANT-1/1 Fuel outer and inner radius at the peak power position.

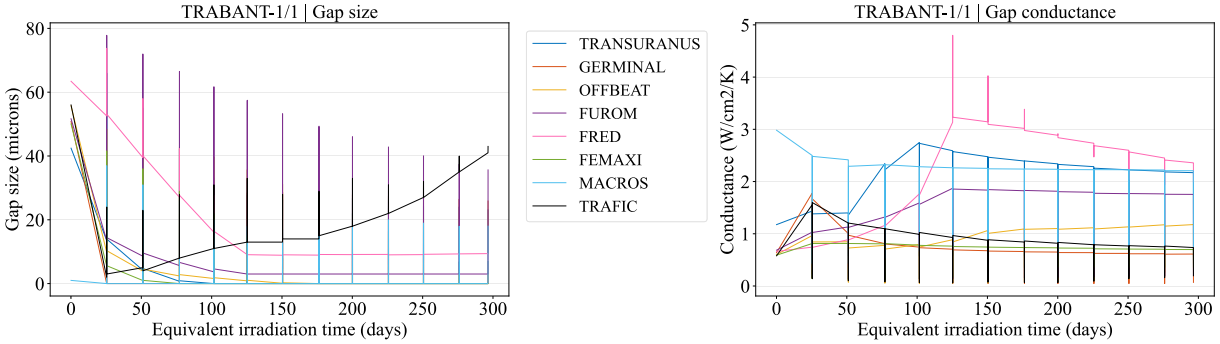

Fig. 10. TRABANT-1/1 Fuel-Cladding gap size (left) and gap conductance (right) at the peak power position.

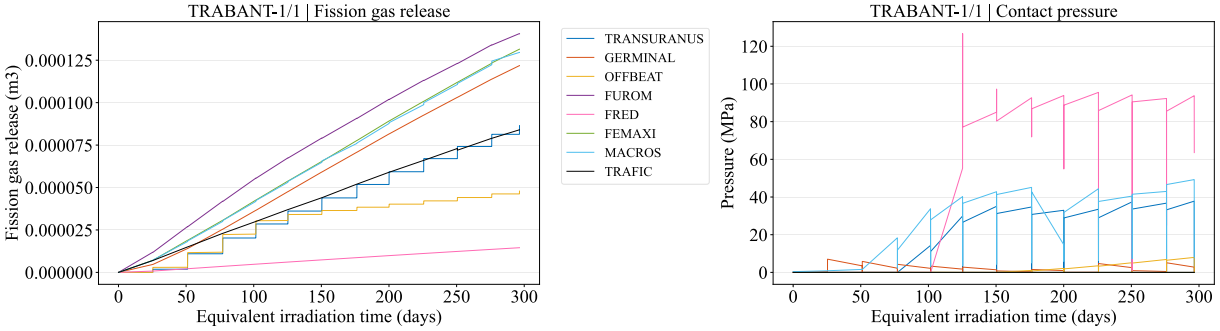

Fig. 11. TRABANT-1/1 FGR (left) and Fuel-Cladding contact pressure (right) at the peak power position.

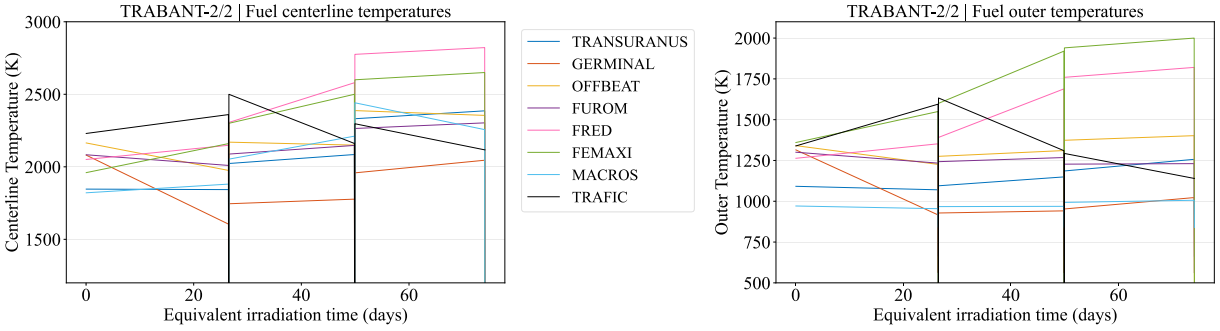

Fig. 12. TRABANT-2/2 Fuel centerline (left) and outer (right) temperatures at the peak power position.

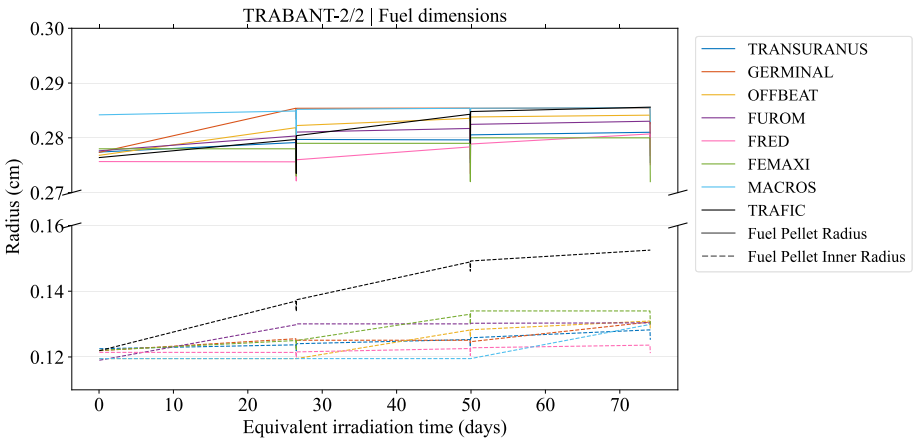

Fig. 13. TRABANT-2/2 Fuel outer and inner radius at the peak power position.

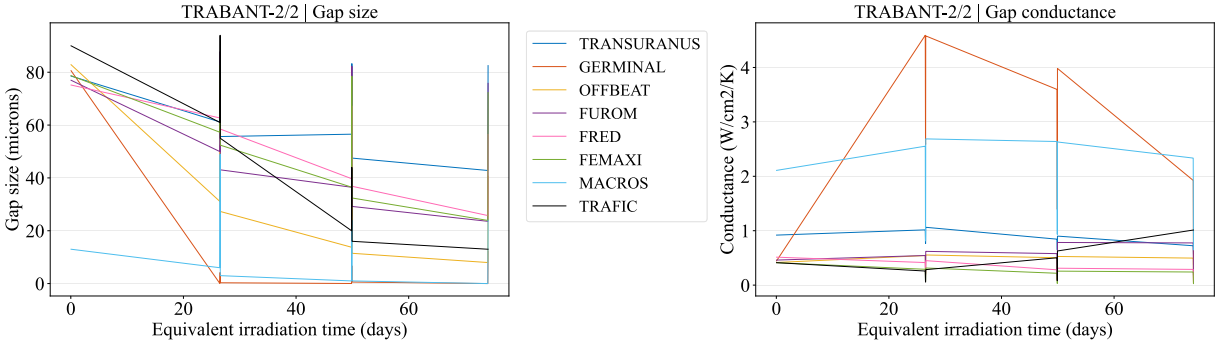

Fig. 14. TRABANT-2/2 Fuel-Cladding gap size (left) and gap conductance (right) at the peak power position.

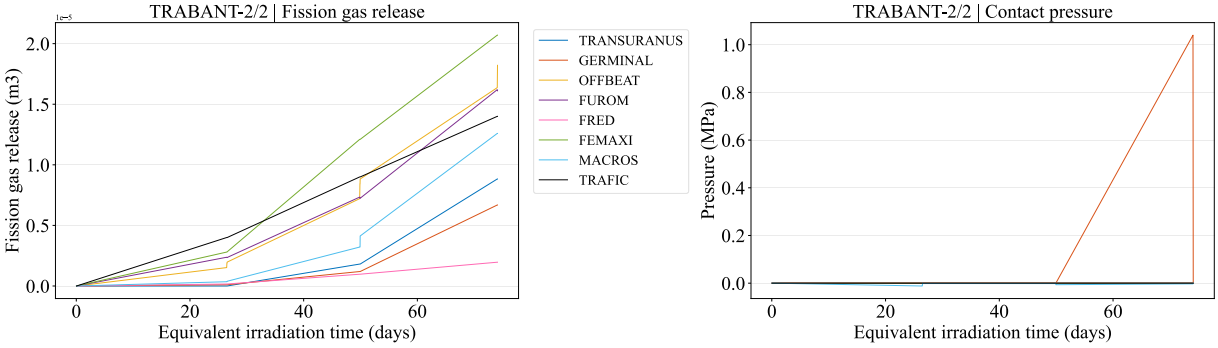

Fig. 15. TRABANT-2/2 FGR (left) and Fuel-Cladding contact pressure (right) at the peak power position.

parameters, assumptions, and modeling choices on the predicted fuel behavior under irradiation. By systematically varying key factors, it identifies the most influential properties and phenomena affecting code outputs. These findings provide a deeper understanding of the sources of variability among codes and offer valuable insights for refining models and correlations in preparation for the second phase of the benchmark.

The influence of nine parameters on the simulation results was tested by means of a sensitivity study which was achieved by applying FPCs to fuel pins explored in this paper.

Three of these parameters were related to the power history:

- Sensitivity to **inter-cycle periods**: The effect of removing the inter-cycle periods is analyzed for all fuel pins, along with the impact of adding a cooling period at the end of the CAPRIX irradiation. In the nominal calculations, power was reduced to zero over one hour at the end of each irradiation cycle and held at that level for several days before the next cycle, simulating experimental conditions.
- Sensitivity to **power variation rate**: This study evaluated the effect of extending the ramp time for start-up and shutdown for each irradiation cycle from 1 h to 12 h for all fuel pins.
- Sensitivity to **power history**: Real power variations during each cycle were applied to TRABANT 1/1 and TRABANT 2/2. Nominal calculations assumed constant power throughout each cycle, while this sensitivity study incorporated actual power fluctuations, including changes in axial power distribution.

The remaining six parameters examined in the sensitivity studies were related to code input, including code models and material properties:

- Clad swelling model: Activated/deactivated.

- Grain size: Varied by ±10 % from the initial grain size.
- Grain growth model: Activated/deactivated.
- JOG (Joint Oxide-Gaine) model: Activated/deactivated.
- Fuel thermal conductivity model: Applied different correlations Philipponneau (Philipponneau, 1992); Magni et al. (Magni et al., 2020) (Magni et al., 2021) and EGIFE (OECD/NEA, 2020).
- Fuel melting temperature model: Magni (Magni et al., 2020; Magni et al., 2021) correlation for the melting temperature.

The sensitivity matrix is reported in Table 2 specifying the codes and pin involved in every parameter studied.

5.1. Sensitivity to power history

Considering the three factors mentioned above: inter-cycle and cooling periods, power variation rates and detailed irradiation history. In general, the power history had a minimal impact on the simulation results, with a few noteworthy exceptions.

For the FRED and FUROM codes, no significant effects were observed in any of the scenarios. In the case of OFFBEAT, the removal of inter-cycle periods led to a notable reduction in FGR for the CAPRIX experiment, while the results for the TRABANT pins showed only minor differences compared to the standard case. The TRANSURANUS code exhibited minimal sensitivity for CAPRIX and TRABANT 2/2, however, for TRABANT 1/1, removing the inter-cycle periods and applying the actual power histories caused a faster fuel-cladding gap dynamic. TRAFIC code showed that while thermal predictions remained similar across different scenarios, mechanical deformation varied, with longer power ramps leading to stronger deformation. GERMINAL revealed significant temperature differences for CAPRIX when inter-cycle periods were removed, attributed to increased helium production during those intervals. For FEMAXI, a sensitivity with respect to gas release in the first irradiation cycle is observed for different power variation rates, likely stemming from initial fuel densification and available time for gases to diffuse out of the fuel.

5.2. Sensitivity to cladding swelling

This sensitivity study assessed the impact of turning off the swelling model for 15-15Ti steel cladding. TRANSURANUS used a conservative swelling model (Luzzi et al., 2014) (higher swelling) instead of the best-estimated one (lower swelling) for three irradiation experiments. The analysis showed minimal effects on most codes, with slight variations in axial and radial expansion in the CAPRIX experiment, where neutron fluence was highest. TRANSURANUS showed a significant reduction of cladding axial expansion in CAPRIX pin. For the TRABANT-1/1 and TRABANT-2/2 pins, the effect is smaller. FUROM showed a slightly larger increase in radial expansion when the swelling model was off. Other parameters were mostly unaffected. Table 3 summarizes the sensitivity of cladding swelling results by code and pin, highlighting variations relative to the nominal simulation results.

5.3. Sensitivity to fuel grain size

This sensitivity study examined the impact of changing grain sizes (6 and 10 μm) by ±10 % based on experimental uncertainty. Larger grains led to lower FGR due to higher retention, while smaller grains caused higher release. The grain size also affected axial behavior, with smaller grains showing larger values. Other parameters were mostly unaffected. Overall, larger grains were preferred for reducing FGR and increasing fuel swelling. No impact was observed with the GERMINAL code. Selected results are presented in the following Tables 4 and 5.

5.4. Sensitivity to grain growth

This study, conducted using GERMINAL and FUROM codes (Kogai, 1989), showed no significant impact on results. For the code FEMAXI, however, a clear influence on fission gas retention is visible with a strong increase in internal gas pressure when the grain size is kept constant. This behavior is clearly illustrated for the CAPRIX pin in Fig. 16.

5.5. Sensitivity to Joint Oxyde-Gaine

This study, using the GERMINAL code, observed that in the sixth cycle of the CAPRIX experiment, the JOG model was activated due to high burnup (see Fig. 17). This caused a sharp increase in thermal conductivity (4 times) in the JOG region (middle of the pellet), leading to a temperature drop of 150 °C at the pellet surface and 200 °C at the center. Similar effects were seen in the TRABANT-1/1 experiment, with increased gap conductance and lower fuel temperature at the end of irradiation. The burnup in the TRABANT-2/2 experiment was too low to activate the JOG model, making sensitivity analysis irrelevant.

These findings highlight the significant impact of JOG modelling on fuel thermal conditions. In this study, sensitivity analyses were conducted exclusively with GERMINAL. Future work should explore the implementation of JOG models in other FPCs to enable comparative analysis and further assess their influence on thermal behavior.

5.6. Sensitivity to fuel thermal conductivity

This sensitivity analysis explored the effect of different fuel thermal conductivity models on pin performance. Various codes used or tested three correlations:

- TRANSURANUS and OFFBEAT: Magni et al. (Magni et al., 2020; Magni et al., 2021) (nominal) and Philipponneau (Philipponneau, 1992) (sensitivity)
- FRED: Philipponneau (Philipponneau, 1992) (nominal) and Magni et al. (Magni et al., 2020) (Magni et al., 2021) (sensitivity)
- GERMINAL: Philipponneau (Philipponneau, 1992) (nominal) and EGIFE (OECD/NEA, 2020) (sensitivity)
- FEMAXI: Philipponneau (Philipponneau, 1992) (nominal), EGIFE (OECD/NEA, 2020) (sensitivity) and Magni et al. (Magni et al., 2020) (Magni et al., 2021) (sensitivity)
- FUROM: Nominal correlation ±10 % (Popov et al., 2000)

Table 2
Sensitivity matrix by codes and parameters (✓: analysis performed, x: analysis not performed).

Parameter	GERMINAL	TRANSURANUS	OFFBEAT	FUROM	TRAFIC	FRED	FEMAXI
Inter-cycle periods	✓✓✓	✓✓✓	✓✓✓	✓✓✓	✓✓✓	✓✓✓	✓✓✓
Power variation rate	✓✓✓	✓✓✓	✓✓✓	✓✓✓	✓✓✓	✓✓✓	✓✓✓
Power history and cooling period	✓✓✓	✓✓✓	✓✓✓	✓✓✓	✓✓✓	✓✓✓	✓✓✓
Cladding swelling	✓✓✓	✓✓✓	✓✓✓	✓xx	xxx	✓✓✓	✓✓✓
Grain size	✓✓✓	✓✓✓	✓✓✓	✓xx	xxx	xxx	✓✓✓
Grain growth	✓✓✓	xxx	xxx	✓xx	xxx	xxx	✓✓✓
JOG model	✓✓✓	xxx	xxx	xxx	xxx	xxx	xxx
Fuel Thermal conductivity	✓✓✓	✓✓✓	✓✓✓	✓xx	xxx	✓✓✓	✓✓✓
Fuel melting temperature	✓✓✓	xxx	✓✓✓	xxx	xxx	xxx	✓✓✓

Table 3
Sensitivity to cladding swelling results by code and pin. Variation relative to the nominal simulation results (%).

Parameter	GERMINAL			TRANSURANUS			OFFBEAT			FRED			FEMAXI			FUROM
	CAP	T-1/1	T-2/2	CAP	T-1/1	T-2/2	CAP	T-1/1	T-2/2	CAP	T-1/1	T-2/2	CAP	T-1/1	T-2/2	CAP
Clad radial expansion	0.3	1.0	0.7	−0.1	0.0	0.0	6.7	0.0	0.0	6.0	2.3	0.0	0.0	0.0	0.0	16.4
Pellet outer radius	0.0	0.0	0.0	−0.1	0.0	0.0	0.0	0.0	0.0	0.0	0.0	0.0	0.0	0.0	0.0	0.0
Clad axial expansion	0.2	0.0	0.0	−23.7	0.0	0.0	2.3	0.0	0.0	0.2	0.2	0.0	−0.2	0.0	0.0	3.5
Fuel axial expansion	−0.2	−3.5	0.0	−0.2	0.0	0.0	0.2	0.0	0.2	0.1	0.1	0.0	0.0	0.0	0.0	0.4
Gap conductance	−0.2	0.1	0.0	0.3	0.0	0.0	−2.7	0.0	11.6	1.0	−0.6	0.0	0.0	0.0	0.0	−2.9
Fuel central temperature	0.0	2.1	0.0	0.0	0.0	0.0	0.3	0.0	−1.9	−0.1	0.0	0.0	0.0	0.0	0.0	0.8

Table 4
Sensitivity to −10% of fuel gran size results by code and pin. Variation relative to the nominal simulation results (%).

Parameter	GERMINAL			TRANSURANUS			OFFBEAT			FEMAXI			FUROM
	CAP	T-1/1	T-2/2	CAP	T-1/1	T-2/2	CAP	T-1/1	T-2/2	CAP	T-1/1	T-2/2	CAP
Fuel axial expansion	0.0	0.0	0.0	0.0	0.0	0.3	0.1	0.1	0.2	0.4	0.1	0.2	0.3
Pellet outer radius	0.0	0.0	0.0	0.0	0.0	0.0	0.0	0.0	0.0	0.0	0.0	0.0	0.0
FGR	0.0	0.0	0.0	0.7	0.2	7.4	2.7	1.5	2.9	3.6	0.6	2.0	1.9
Internal pressure	0.0	0.0	0.0	0.6	0.2	3.5	2.6	1.4	1.7	2.7	0.5	1.4	1.9
Fuel central temperature	0.0	0.0	0.0	0.0	0.0	0.3	0.0	0.4	−0.2	0.0	0.0	0.0	0.0

Table 5
Sensitivity to + 10 % of fuel gran size results by code and pin. Variation relative to the nominal simulation results (%).

Parameter	GERMINAL			TRANSURANUS			OFFBEAT			FEMAXI			FUROM
	CAP	T-1/1	T-2/2	CAP	T-1/1	T-2/2	CAP	T-1/1	T-2/2	CAP	T-1/1	T-2/2	CAP
Fuel axial expansion	0.0	0.0	0.0	0.0	0.0	−0.3	−0.1	−0.1	−0.3	−0.3	0.0	−0.2	−0.3
Pellet outer radius	0.0	0.0	0.0	0.0	0.0	0.0	0.0	0.0	0.0	0.0	0.0	0.0	0.0
FGR	0.0	0.0	0.0	−0.4	−0.1	−5.8	−3.2	−1.5	−2.6	−2.2	−0.6	−1.6	−2.3
Internal pressure	0.0	0.0	0.0	−0.4	−0.1	−2.7	−3.0	−1.5	−1.5	−2.7	−0.5	−1.1	−2.2
Fuel central temperature	0.0	0.0	0.0	0.0	0.0	−0.1	0.0	−0.4	0.3	−0.1	0.0	0.0	0.0

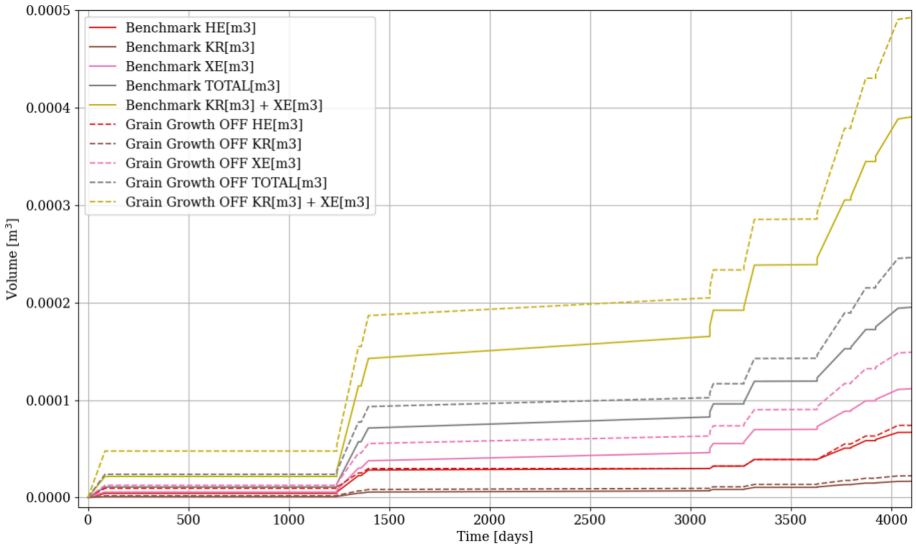

Fig. 16. CAPRIX Grain growth model sensitivity: Fission gas release using FEMAXI.

TRANSURANUS and FRED outcomes for this sensitivity analysis were similar. Results showed that the Magni et al. (Magni et al., 2020; Magni et al., 2021) model predicted fuel center temperatures 50–70 °C higher than the Philipponneau (Philipponneau, 1992) model due to stronger burnup degradation of fuel thermal conductivity. However, this temperature difference had little effect on other key parameters, like gap conductance, which is influenced by both gap size and FGR.

In FRED code, for TRABANT 1/1 and TRABANT 2/2, the Magni et al. (Magni et al., 2020; Magni et al., 2021) correlation resulted in higher gap conductance compared to Philipponneau (Philipponneau, 1992). In TRANSURANUS, the gap conductance was lower. The competing effects of increased FGR and fuel swelling caused variations in results across pins.

For OFFBEAT, the Magni et al. (Magni et al., 2020; Magni et al., 2021) correlation predicted higher centerline temperatures for the CAPRIX pin but showed the opposite behavior for the TRABANT pins.

With GERMINAL, the Philipponneau (Philipponneau, 1992) model led to higher temperatures and more FGR in CAPRIX and TRABANT 2/2,

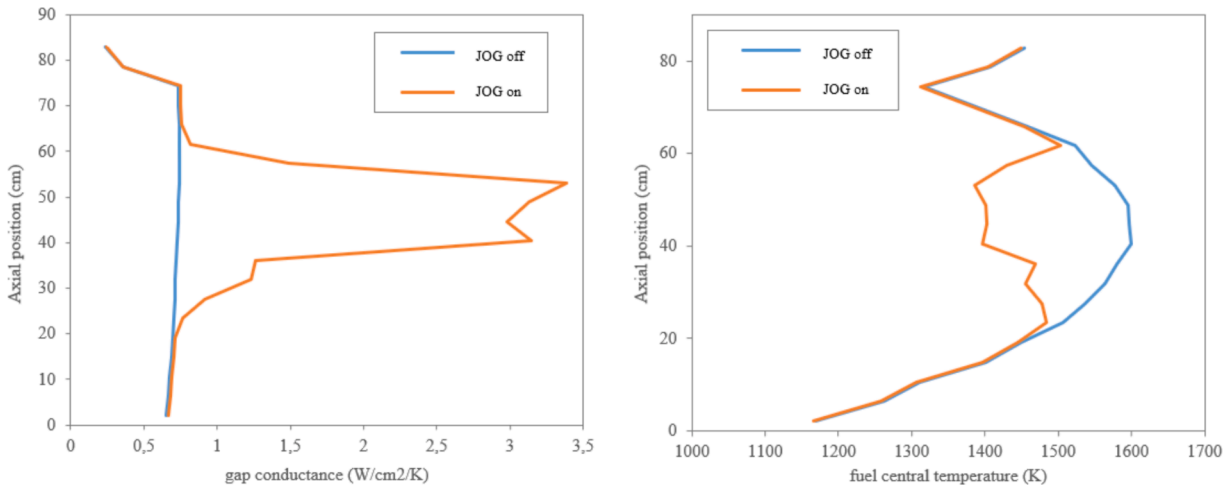

Fig. 17. CAPRIX Influence of the JOG model at end of irradiation: gap conductance (left) and the central fuel temperature (right), as predicted by the GERMINAL.

while the EGIFE model produced lower initial temperatures and pressure, but higher values later in irradiation for TRABANT 1/1.

The FEMAXI calculations align with most observations, showing a progressive increase in fuel inner temperature from the EGIFE case (OECD/NEA, 2020) (lowest temperature) to the Philipponneau case (Philipponneau, 1992) and the Magni et al. cases (Magni et al., 2020; Magni et al., 2021) (highest temperature). This trend is reflected in the corresponding fuel swelling and FGR.

Since the influence of different correlations varies across codes, a focused comparison is presented if Fig. 18 for clarity. The following figures focus on a direct comparison of centerline temperature differences for two cases: GERMINAL (comparing Philipponneau vs. EGIFE) and TRANSURANUS (comparing Magni et al. vs. Philipponneau) in the CAPRIX simulation. These focused comparisons emphasize how the choice of thermal conductivity model influences the predicted thermal behavior and, by extension, other performance parameters in each simulation code.

5.7. Sensitivity to fuel melting temperature

Results were generated using GERMINAL, OFFBEAT and FEMAXI codes. The OFFBEAT study examined the impact of activating the melting temperature criterion for MOX fuel (Magni et al. correlation (Magni et al., 2020), but no significant differences were observed, as the melting temperature was not reached in any of the pins. Similarly, GERMINAL performed a sensitivity analysis by lowering the melting temperature by 150 K. However, this also resulted in no appreciable changes from the nominal results since fuel melting did not occur in any of the cases. The same results are obtained with FEMAXI: since melting temperature is not reached, there is no difference with respect to the sensitivity case.

Overall, the analysis confirms that under the current operating conditions, variations in the fuel melting temperature have no effect on the simulation outcomes because the fuel temperatures do not approach the melting point.

6. Discussion

The involvement of different FPCs in this work is an excellent opportunity to highlight significant divergences between codes when modeling MOX fuel with high Pu content. This is particularly evident at elevated Pu levels, such as those found in CAPRIX, TRABANT-1/1 and TRABANT-2/2. Many codes attempt to simulate complex behaviors that, in some cases, extend beyond their validation domains. The benchmark results presented in Section 4 highlight notable variations, particularly in predicted pellet temperatures. Both centerline and outer pellet temperatures differ significantly across the codes, likely due to discrepancies in fuel thermal conductivity, thermal expansion, relocation, and gap conductance models.

Complementary to the reference results, the sensitivity analyses

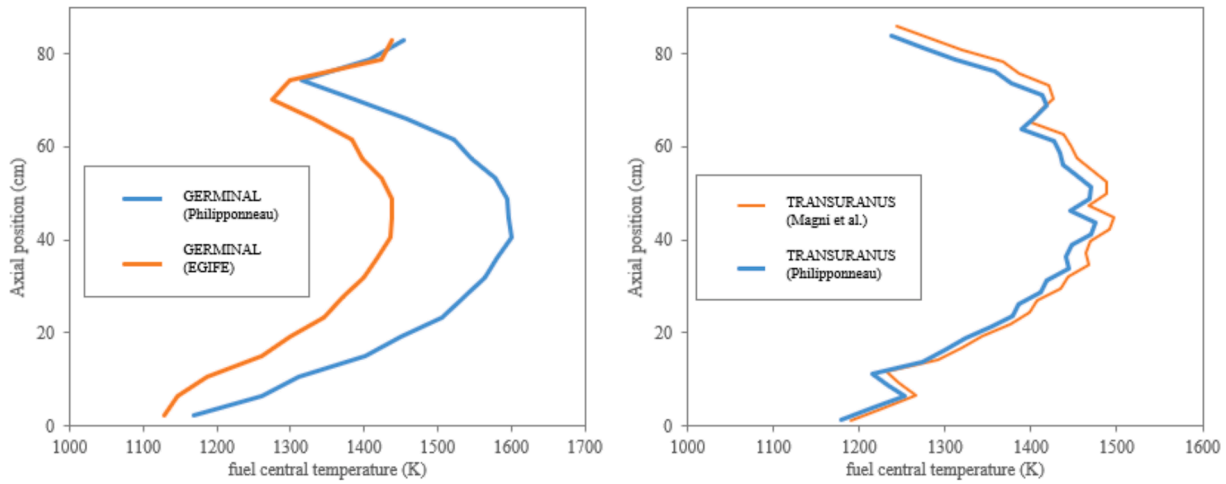

Fig. 18. Fuel central temperature at end of irradiation: GERMINAL (left) and TRANSURANUS (right).

performed in this study provide key insights into the sources of these discrepancies. Temperature predictions at the beginning of irradiation (see Table 6) indicate that while absolute centerline and outer pellet temperatures vary, the temperature gradients within the fuel remain relatively consistent. The sensitivity analysis of thermal conductivity further suggests that differences in how each code model's conductivity degradation with burnup have a significant impact on the results. This indicates that the primary source of divergence lies in the material property definitions of the fuel and cladding, rather than in fundamental modelling approaches. However, differences in gap conductance treatments, particularly the influence of gap dynamics and FGR, further contribute to the observed variations in temperature profiles (see Section 4).

The thermal conductivity sensitivity assessment revealed notable differences in how codes account for its impact on fuel temperature, contrasting with the relatively minor effect on melting temperatures under the current operating conditions, where fuel temperatures remain well below melting. These discrepancies underscore the need for harmonizing critical thermal properties, such as thermal conductivity, across all codes to ensure more consistent predictions.

The sensitivity analysis on JOG further confirms that fuel thermal conductivity and gap conductance play a dominant role in codes-to-code discrepancies. Codes like GERMINAL, which includes a JOG model, predict distinct temperature regimes compared to those without it. The absence of a JOG model in most codes has been identified as a major source of divergence.

Furthermore, the sensitivity tests demonstrated that certain parameters, such as grain size, have minimal influence on FGR and internal gas pressure in some codes, even when varied by ±10 %. This suggests that the models governing grain growth and related phenomena may require refinement or a more integrated treatment to better capture their effects.

Overall, these analyses confirm that the observed discrepancies stem primarily from differences in material property definitions and implementations, rather than from fundamental modelling divergences, except in cases where certain behaviors are not modelled at all. To address this, the next phase of the benchmark should prioritize the standardization of thermal property definitions across all codes to isolate remaining sources of disagreement. Additionally, further comparisons with experimental data should be conducted, with particular emphasis on evaluating GERMINAL temperature predictions relative to other codes, given that it is the only one incorporating a JOG model. Even simplified JOG models should be considered for integration into all codes.

In fact, the primary goal of phase II of this benchmark exercise will be to expand the validation of all the involved codes, not only with respect to Pu content but also by enhancing their capability to model key phenomena under these irradiation conditions. A notable example uncovered during this study is the absence of a JOG model in most of the codes. Furthermore, this blind benchmark serves as a valuable reference for estimating the expected uncertainty in FPC outputs, providing essential information for defining safety margins in the design of irradiations involving high-Pu MOX fuel. These efforts will contribute to more reliable and accurate predictions for safety–critical scenarios.

7. Conclusion

Based on the results and analysis from the blind phase of this benchmark study, the most relevant conclusions about the FPCs on CAPRIX, TRABANT-1/1 and TRABANT-2/2 are summarized as follows:

- The aimed of the blind phase, a code-to-code comparison, revealed significant discrepancies in results. Despite the alignment of key input specifications such as LHR, fast neutron flux, outer cladding temperature, pin geometries and fuel compositions across the different codes. These discrepancies highlight the varying models currently employed for critical fuel and cladding properties, as well as the different phenomena and weight simulated by each code.
- This blind benchmark phase has proven valuable in identifying variations in safety-relevant metrics such as fuel and cladding temperatures, fuel restructuring, gap evolution, contact pressure, FGR and inner pin pressure. These insights are essential for understanding differences in how each code models the thermal–mechanical behavior of the fuel pin under irradiation.
- Complementary sensitivity analyses conducted alongside the reference code results provided a clear evaluation of the impact of different input parameters, assumptions and modeling choices. Through these analyses, the most critical properties and phenomena have been identified, providing a clear direction for future modeling improvements. Of particular interest, the fuel thermal conductivity, melting temperature, cladding swelling, initial fuel grain size and Joint Oxide-Gaine formation.
- This work emphasizes the importance of accurate irradiation history, rather than average values, as it significantly influences the fuel temperature regime and related phenomena like fuel restructuring and thermal expansion, which drive gap dynamics. Additionally, the gap conductance is identified as a key driver of the pin's thermal–mechanical performance, is modeled very differently across the codes and remains underexplored in the sensitivity analyses.
- Looking forward to the second phase of this benchmark, to reduce discrepancies and improve the predictive capabilities of FPCs, it is crucial to establish the most reliable input settings and correlations. This is essential, especially as the focus shifts towards simulating fuels with higher plutonium contents (up to 60 %) and more demanding irradiation conditions.

The next critical step in the benchmark activity will involve validating the code results against experimental data from CAPRIX, TRABANT 1/1 and TRABANT 2/2 within the PuMMA framework. This validation will demonstrate the codes' applicability to FR irradiation conditions with high LHRs and MOX fuels with high plutonium contents.

Table 6
Temperature differences at beginning of irradiation for the three pins simulated by all codes.

	Temp. (K)	TRANSURANUS	GERMINAL	OFFBEAT	FUROM	FRED	FEMAXI	MACROS	TRAFIC	Avg.	Std. Dev.
CAP	Inner	1836	2144	2175	2132	2059	2130	1776	2429	2085	204
	Outer	1027	1294	1295	1263	1205	1300	885	1305	1197	157
	Gradient	809	849	879	870	854	830	892	1124	888	99
T-1/1	Inner	2609	2752	2794	2646	2881	2783	2495	2851	2726	132
	Outer	1227	1479	1500	1444	1475	1544	1043	1460	1396	171
	Gradient	1382	1273	1294	1202	1406	1239	1452	1391	1330	90
T-2/2	Inner	1846	2080	2165	2083	2051	1960	1821	2230	2029	145
	Outer	1092	1315	1341	1301	1263	1360	971	1339	1248	140
	Gradient	755	766	824	782	787	600	850	891	782	86

Declaration of Generative AI and AI-assisted technologies in the writing process

During the preparation of this work the author(s) used AI-assisted technologies to improve readability and language. After using this tool/service, the author(s) reviewed and edited the content as needed and take(s) full responsibility for the content of the publication.

CRediT authorship contribution statement

D. Jaramillo-Sierra: Writing – review & editing, Writing – original draft, Visualization, Validation, Methodology, Investigation, Formal analysis, Data curation, Conceptualization. **M. Stefanowska-Skrodzka:** Writing – review & editing, Writing – original draft, Data curation, Conceptualization. **J. Lavarenne:** Writing – review & editing, Writing – original draft, Visualization, Data curation, Conceptualization. **E. Deveaux:** Writing – review & editing, Writing – original draft, Visualization, Validation, Methodology, Formal analysis, Data curation, Conceptualization. **E. Brunetto:** Writing – review & editing, Writing – original draft, Visualization, Validation, Methodology, Investigation, Formal analysis, Data curation, Conceptualization. **V. Matocha:** Writing – review & editing, Writing – original draft, Visualization, Validation, Methodology, Investigation, Formal analysis, Data curation, Conceptualization. **A. Magni:** Writing – review & editing, Writing – original draft, Visualization, Validation, Methodology, Investigation, Formal analysis, Data curation, Conceptualization. **K. Sturm:** Writing – review & editing, Writing – original draft, Methodology, Investigation, Formal analysis, Data curation, Conceptualization. **K. Mikityuk:** Writing – review & editing, Writing – original draft, Methodology, Data curation, Conceptualization. **Y. Wang:** Writing – review & editing, Writing – original draft, Methodology, Investigation, Data curation. **A. Jiménez-Carrascosa:** Writing – review & editing, Writing – original draft, Visualization, Validation, Methodology, Investigation, Formal analysis, Data curation. **J. Gado:** Writing – review & editing, Formal analysis, Conceptualization. **B. Burger:** Writing – review & editing, Methodology, Data curation, Conceptualization. **V. Blanc:** Writing – review & editing, Writing – original draft, Visualization, Supervision, Methodology, Investigation, Data curation, Conceptualization. **V. Dupont:** Writing – review & editing, Writing – original draft, Visualization, Methodology, Investigation, Formal analysis, Data curation, Conceptualization. **L. Argeles:** Writing – review & editing, Data curation, Conceptualization. **B. Perrin:** Writing – review & editing, Data curation, Conceptualization. **G. Michel:** Writing – review & editing, Methodology, Conceptualization. **A. Scolaro:** Writing – review & editing, Writing – original draft, Supervision, Methodology, Investigation, Data curation. **C. Fiorina:** Funding acquisition, Conceptualization. **J. Peltonen:** Writing – review & editing, Conceptualization. **A. Del Nevo:** Writing – review & editing, Writing – original draft, Supervision, Data curation, Conceptualization. **L. Luzzi:** Writing – review & editing, Supervision, Project administration, Conceptualization. **D. Pizzocri:** Writing – review & editing, Supervision, Methodology, Investigation, Data curation, Conceptualization. **S. Lemehov:** Writing – review & editing, Methodology, Data curation, Conceptualization. **S. Bebjak:** Writing – review & editing, Writing – original draft, Validation, Methodology, Investigation, Formal analysis, Data curation, Conceptualization. **T. Chrebet:** Writing – review & editing, Methodology, Investigation, Data curation, Conceptualization. **C. Strmensky:** Writing – review & editing, Writing – original draft, Validation, Methodology, Investigation, Formal analysis, Data curation, Conceptualization.

Declaration of competing interest

The authors declare that they have no known competing financial interests or personal relationships that could have appeared to influence the work reported in this paper.

Acknowledgements

This work has received funding from the European Union's Horizon 2020 research and innovation program through the PuMMA Project under grant agreement No 945022.

Appendix A. Codes material properties

This appendix presents the material property references provided by the various codes involved in the benchmark activity, as detailed in Table 7. However, some models and correlations could not be retrieved due to limited data sharing.

Table 7
Material properties reported by the different codes.

		Code							
Model		FUROM	GERMINAL	OFFBEAT	TRANSURANUS	FRED	MACROS	FEMAXI	TRAFIC
Plenum gas homogenisation law		MATPRO (NUREG/CR-0497, TREE-1280, Rev. 2, 1981)	Arnaud and Roche's model (Arnaud and Roche, 1977).	FRAPCON (Lassmann and Hohlefeld, , 1987)	URGAS model (Lassmann and Hohlefeld, 1987)	–	–		Proprietary
Conductivity	Fuel	Popov et al. (Popov et al., 2000)	Philipponneau (Philipponneau, 1992).	Magni (Magni et al., 2020)	Magni (Magni et al., 2020)	Philipponneau (Philipponneau, 1992).	–	Philipponneau (Philipponneau, 1992).	
	Cladding	Többe (Többe, 1975)	Böhler et al. (R. Böhler, 2014).	Többe (Többe, 1975)	Többe (Többe, 1975)	Luzzi et al. (Luzzi et al., 2013)	–	–	
Melting point	Fuel	Pesl et al. (Pesl et al., 1987)	Böhler et al. (Böhler, 2014).	Magni (Magni et al., 2020)	Magni (Magni et al., 2020)	MATPRO (Sari, 1986)	–	–	
	Cladding	ASM (ASM)	Maloy et al. (Maloy et al., 2020).		Schumann (Beyer et al, , 1975)	Luzzi et al. (Luzzi et al., 2013)	–	–	
Emissivity	Fuel	Beyer et al (C. E. Beyer e. al, , 1975):	Arnaud et Roche (Arnaud and Roche, 1977).	RELAP (ESNII+ Deliverable	Fink (J. K. Fink, , 1981)	MATPRO (Sari, 1986)	–	–	

(continued on next page)

Table 7 (*continued*)

		Code							
Model		FUROM	GERMINAL	OFFBEAT	TRANSURANUS	FRED	MACROS	FEMAXI	TRAFIC
				D7.5.1, 2017)					
	Cladding	Beyer et al (Beyer et al., 1975):	Maloy et al. (Maloy et al., 2020).	0.809	0.8	Luzzi et al. (Luzzi et al. 2013.)	–	–	
Thermal expansion	Fuel	Popov et al. (Popov et al., 2000)	Reference (Chauvin et al., 2023).	Lemehov (Petrovic et al., 1977)	Lemehov (Petrovic et al., 1977)	MATPRO (Sari, 1986)	–	–	
	Cladding	Bisor (Bisor, 2018)	Maloy et al. (Lainet et al., 2019).	Gehr (Catalogue des propriétés des oxydes mixtes (UPu) O2, 1977)	Gehr (Catalogue des propriétés des oxydes mixtes (UPu)O2, 1977)	Luzzi et al. (Luzzi et al., 2013.)	–	–	
Elastic coefficients: Young Modulus	Fuel	ESNII + Deliverable D7.5.1 (ESNII+ Deliverable D7.5.1, 2017)	Martin's law (AGT 01 01 01, 1990) modify depending on the burn-up, deduced from Marchetti et al.,'s correlation (Marchetti et al., 2017).	Lemehov (Petrovic et al., 1977)	Lemehov (Petrovic et al., 1977)	MATPRO (Sari, 1986)	–	–	
	Cladding	Bisor (Bisor, 2018)	Maloy et al. (Maloy et al., 2020).	Többe (Többe, 1975)	Többe (Többe, 1975) and Pesl et al. (Pesl et al., 1987)	Luzzi et al. (Luzzi et al., 2013)	–	–	
Elastic coefficients: Poisson's ratio	Fuel	ESNII + Deliverable D7.5.1 (ESNII+ Deliverable D7.5.1, 2017)	The Poisson's ratio of the mixed oxide is evaluated using the Young's modulus and the shear modulus of dense UO2	MATPRO (Bisor, 2018)	nu = 0.32	MATPRO (Sari, 1986)	–	–	
	Cladding	ASM (ASM)	Maloy et al. (Maloy et al., 2020).	Többe (Többe, 1975)	Többe (Többe, 1975) and Pesl et al. (Pesl e. al., 1987)	Luzzi et al. (Luzzi and S. Lorenzi és D. Pizzocri, , 1493, 2013.)	–	–	
Yield stress	Fuel	ESNII + Deliverable D7.5.1 (ESNII+ Deliverable D7.5.1, 2017)	Petrovic et al. (Petrovic et al., 1977), Radford and Terwilliger (Radfordés and Terwilliger, 1975) in agreement with (Catalogue des propriétés des oxydes mixtes (UPu) O2, 1977)	300 MPa	Canonet (Canonet et al., 1971)	–	–	–	
	Cladding	ASM (ASM)	Maloy et al. (Maloy et al., 2020).	926 MPa	Többe (Többe, 1975)	Luzzi et al. (Luzzi et al., 2013.)	–	–	
Rupture stress	Fuel		From (Catalogue des propriétés des oxydes mixtes (UPu) O2, 1977).	–	–	–	–	–	
	Cladding	Luzzi et al. (Luzzi et al., 2013)	Maloy et al. (Maloy et al., 2020).	–	Többe (Többe, 1975)	Luzzi et al. (Luzzi et al., 2013)	–	–	
Densification law	Fuel	GAPCON-THERMAL (Beyer et al., 1975)	–	FRAPCON (Lassmann and Hohlefeld, 1987)	Olander with the model of Dienst (Olander, 1976)	–	–	–	
Swelling	Cladding	Luzzi et al. (Luzzi et al., 2013.)			Luzzi (Luzzi et al., 2014)	–	–	–	
Irradiation creep	Fuel	ESNII + Deliverable D7.5.1 (ESNII+ Deliverable D7.5.1, 2017)	Sari's model (Sari, 1986) with the sensitivity of creep to grain size by Guérin's law (Guérin, 1983).	Dienst (Dienst, 1977)	Malygin (Malygin et al., 2010)	MATPRO (Sari, 1986)	–	–	

(*continued on next page*)

Table 7 (*continued*)

Model	Code							
	FUROM	GERMINAL	OFFBEAT	TRANSURANUS	FRED	MACROS	FEMAXI	TRAFIC
Cladding	Luzzi et al. (Luzzi et al., 2013)		Többe (Többe, 1975)	Többe (Többe, 1975)	Luzzi et al. (Luzzi et al., 2013)	–	–	

Data availability

Data will be made available on request.

References

"Catalogue européen des propriétés de l'oxyde mixte (UPu)O2 Fast Reactor Data Manual, Issue 1," edited by AGT 01 01 01, 1990.

Arnaud, A.M., Roche, L. 1977. "Échanges thermiques dans une lame gazeuse Coefficient d'échange thermique entre combustible et gaine," 1977.

"ASM.matweb.com".

Beyer, C.E., et al. 1975. "GAPCON-THERMAL-2: A Computer Program for Calculating the Thermal Behaviour of an Oxide Fuel Rod," BATTELLE Pacific Northwest Laboratories, 1975.

Bisor, C., 2018. Data on AIM1 cladding in support of ALLEGRO project. Private Commun.

Bisor, C. 2018. "AIM1 dataset," internal material, June 2018.

Böhler, R., et al., 2014. Recent advances in the study of the UO_2-PuO_2 phase diagram at high temperatures. J. Nucl. Mater. 448, 330–339.

Canonet, R.F., et al., 1971. Deformation of UO_2 at high temperatures. J. Am. Ceram. Soc. 54.

"Catalogue des propriétés des oxydes mixtes (UPu)O2," D.M.E.C.N. / D.E.C.Pu / S.E.A.M. A. – Note Technique N° 191, 1977.

Chauvinés, N., et al., „Recommendations on fuel properties for fuel performance codes," OECD/NSC/WPFC/EGIFE, NT 23-008-A,, 2023.

Di Marcello, V., Schubert, A., van de Laar, J., Van Uffelen, P., 2012. Extension of the TRANSURANUS plutonium redistribution model for fast reactor performance analysis. Nucl. Eng. Des. 248, 149–155.

Di Marcello, V., Rondinella, V., Schubert, A., van de Laar, J., Van Uffelen, P., 2014. Modelling actinide redistribution in mixed oxide fuel for sodium fast reactors. Prog. Nucl. Energy 72, 83–90.

"Catalog on MOX properties for fast reactors," ESNII+ Deliverable D7.5.1, 2017.

European Commission, 2021. TRANSURANUS Handbook. JRC - Joint Research Centre, Karlsruhe, Germany.

Fink, J.K., et al., 1981. Thermophysical properties of uranium dioxide. J. Nucl. Mater. 102, 17–25.

Guérin, Y. 1983. "SLHA/GC 83-2011".

Hsieh, T., Billone M., Rest, J. 1982. "Development and verification of the LIFE-GCFR computer code for predicting gas-cooled fast-reactor fuel-rod performance," ANL-84-1, http://www.iaea.org/inis/collection/NCLCollectionStore/_Public/14/738/14738447.pdf.

[Online]. Available: http://www-cast3m.cea.fr/. [Accessed 11 10 2022].

Kogai, T., et al., 1989. In-pile and out-of-pile grain growth behavior of sintered UO_2 and $(U,Gd)O_2$ pellets. J. Nucl. Sci. Techn. 26 (8), 744–751.

Lainet, M., Michel, B., Dumas, J.-C., Pelletier, M., Ramière, I., 2019. GERMINAL, a fuel performance code of the PLEIADES platform to simulate the in-pile behaviour of mixed oxide fuel pins for sodium-cooled fast reactors. J. Nucl. Mater. 516, 30–53.

Lassmann, K., 1992. TRANSURANUS: a fuel rod analysis code ready for use. J. Nucl. Mater. 188 (C), 295–302.

Lassmann, K., Hohlefeld, F. 1987. "The revised URGAP model to describe the gap conductance between fuel and cladding," Nucl. Eng. Des. %1. kötetVolume 103, %1. szám2, pp. 215-221.

Lavarenne, J., Lainet, M., Perrin, B., Mikityuk, K., Murphy, C. 2019. "Final report on Fuel Performance and Gap Conductance," ESFR-SMART.

Lemehov, S., 2020. New correlations of thermal expansion and Young's modulus based on existing literature and new data. INSPYRE Deliverable D6, 3.

Luzzi, L., Cammi, A., Di Marcello, V., Lorenzi, S., Pizzocri, D., Van Uffelen, P., 2014. Application of the TRANSURANUS code for the fuel pin design process of the ALFRED reactor. Nucl. Eng. Des. 277, 173–187.

Luzzi, L., Lorenzi, S., Pizzocri, D. 2013. "Modeling and analysis of nuclear fuel pin behavior for innovative lead cooled FBR," CERSE-POLIMI RL 1493.

Magni, A., Barani, T., Del Nevo, A., Pizzocri, D., Staicu, D., Van Uffelen, P., Luzzi, L., 2020. Modelling and assessment of thermal conductivity and melting behaviour of MOX fuel for fast reactor applications. J. Nucl. Mater. 541, 152410.

Magni, A., Del Nevo, A., Luzzi, L., Rozzia, D., Adorni, M., Schubert, A., Van Uffelen, P. 2021. "The TRANSURANUS fuel performance code," in Nuclear Power Plant Design and Analysis Codes - Development, Validation and Application, Woodhead Publishing Series in Energy, Elsevier, 2021, pp. 161-205, Chap. 8, Vol. III.

Magni, A., Luzzi, L., Pizzocri, D., Schubert, A., Van Uffelen, P., Del Nevo, A., 2021. Modelling of thermal conductivity and melting behaviour of minor actinide-MOX fuels and assessment against experimental and molecular dynamics data. J. Nucl. Mater. 557, 153312.

Maloy, S., et al., 2020. "Recommendations cladding materials properties for fuel performance codes," 2020.

Malygin, et al., 2010. Atomic Energy 108.

Marchetti, M., et al., 2017. J. Nucl. Mater. 494, 322–329.

Mikityuk, K., Shestopalov, A., 2011. FRED fuel behaviour code: main models and analysis of Halden IFA-503.2 tests. Nucl. Eng. Des. 241, 2455–2461.

Nindiyasari, F., Til, S.v., Charpin-Jacobs, F. 2022. "PUMMA project - D2.1.2 - Reconstruction of the irradiation history of TRABANT 1/1".

"MATPRO-Version 11 (revision 2) A Handbook of Material Properties for Use in the Analysis of Light Water Reactor Fuel Rod Behaviour," NUREG/CR-0497, TREE-1280, Rev. 2,, 1981.

OECD/NEA, "Expert Group on Innovative Fuel Elements (EGIFE)," 2020. [Online]. Available: https://www.oecd-nea.org/jcms/pl_22428/expert-group-on-innovative-fuels-egif.

Okawa, T., Tatewaki, I., Ishizu, T., Endo, H., Tsuboi, Y., Saitou, H., 2015. Fuel behavior analysis code FEMAXI-FBR development and validation for core disruptive accident. Prog. Nucle. Energy 82, 80–85.

Olander, D.R. 1976. "Fundamental Aspects of Nuclear Reactor Fuel Elements".

R. Pesl és e. al., „SATURN-S, Ein Programmsystem zur Beschreibung des thermomechanischen Verhaltens von Kernreaktorbrennstäben unter Bestrahlung," Kernforschungszentrum Karlsruhe, KfK 4272, 1987.

Petrovic, J.J., et al. 1977. "report LA-6529," Los Alamos National Laboratory, April 1977.

Philipponneau, Y., 1992. Thermal conductivity of (U, Pu)O2-x mixed oxide fuel. J. Nucl. Mater. 188, 194–197.

Popov, S.G., Garbajo, J.J., Ivanov, V.K., Yoder, G.L. 2000. "Thermophysical Properties of MOX and UO2 Fuels Including the Effects of Irradiation," ORNL/TM-2000/351 report.

"Grant Agreement - 945022 - PUMMA; Annex 1: Description of the action".

K. C. Radford G. R. Terwilliger, Journal of the American Ceramic Society,, %1. kötetVolume 58, 1975.

Sari, C., 1986. J. Nucl. Mater. 137, 100–106.

"SCDAP/RELAP5-3D© Code Manual, Volume 4: MATPRO - A library of materials properties for Light-Water-Reactor accident analysis," INEEL/EXT-02-00589, Revision 2.2, October 2003.

Scolaro, A., Clifford, I., Fiorina, C., Pautz, A., 2020. The OFFBEAT multi-dimensional fuel behavior solver. Nucl. Eng. Des. 358.

Sundman, B., Kattner, U.R., Sigli, C., Stratmann, M., Tellier, R., Palumbo, M., Fries, S.G., 2016. The OpenCalphad thermodynamic software interface. Comput. Mater. Sci. 125, 188–196.

S. v. Til, A. Fedorov and F. Charpin-Jacobs, "PUMMA project - D2.1.3 - Reconstruction of the irradiation history of TRABANT 2/2," 2022.

Többe, H. 1975. "Das Brennstabrechenprogramm IAMBUS zur Auslegung von SchellbrüterBrennstäben," Interatom. Technischer Bericht, ITB 75.65.

T. Tverberg, "Mixed-oxide (MOX) Fuel Performance Benchmark - Summary of the Results for the Halden Reactor Project MOX Rods, OECD Halden Reactor Project," NEA/NSC/DOC, 2007.

Van Uffelen, P., Schubert, A., Luzzi, L., Barani, T., Magni, A., Pizzocri, D., Lainet, M., Marelle, V., Michel, B., Boer, B., Lemehov, S., Del Nevo, A., 2020. Incorporation and verification of models and properties in fuel performance codes. INSPYRE Deliverable D7, 2.

Venard, C., Deveaux, E. 2021. "Pumma Project, D2.1.1 CAPRIX irradiation conditions in Phenix".

Venard, E.D.C. 2021. "CAPRIX irradiation conditions in PHENIX - D2.1.1 Version N°1".

Waltar, A., Reynolds, A. 1981. Fast Breeder Reactors,, Pergamon Press, (ISBN: 9780080259833) pp.265-267.

Dienst, W.. Irradiation-Induced Creep of Ceramic Nuclear Fuels, Pages 1-8. https://doi.org/10.1016/B978-0-7204-0572-9.50005-8.